

Thermal coupling of methane. A comparison between kinetic model data and experimental data

Ola Olsvik ^a and Francis Billaud ^{*,b}

^a SINTEF Applied Chemistry, N-7034 Trondheim (Norway)

^b Département de Chimie-Physique des Réactions, URA n°328 CNRS, INPL-ENSIC, 1 rue Grandville, BP 451, 54001 Nancy Cédex (France)

(Received 31 March 1993; accepted 18 May 1993)

Abstract

Thermal coupling of methane was investigated in a tubular flow reactor in the temperature range 1200–1500°C at atmospheric pressure.

The main products observed were ethane, ethene, ethyne, benzene and “coke”. A mechanistic simulation model was developed for this process. The kinetic scheme consists of 32 reversible free radical reactions and one irreversible free radical reaction. The model data provide good agreement with experimental data for the conditions being studied.

A sensitivity analysis was used to find the main free radical reactions in the formation and consumption of the reported products.

INTRODUCTION

Thermal coupling of methane has been extensively studied in the literature. The latest review on the subject by Billaud et al. [1] includes the most important results obtained since 1960. This review shows that few authors have carried out experiments in the temperature range 1000–1500°C and only a few simulations have been presented.

Ranzi et al. [2] studied the thermal coupling of methane at high temperature (1400–1500°C). They used a simplified kinetic scheme where only reactions of relative importance (higher than 1%) in formation (or disappearance) of the main molecular species are included. Their kinetic model involves reversible radical reactions and some purely reversible molecular reactions. Ranzi et al. [2] concluded that high temperatures improve the selectivity of ethyne and maxima in the yields are achieved at

* Corresponding author.

lower contact times. The selectivity of ethene was shown to decrease with increasing temperature. Hydrogen dilution decreased the reactivity of the system and improved the C_2 yields and selectivities.

The present work is a study of the pyrolysis of methane at high temperatures (1200–1500°C) both at high and low conversions, and we have tried to use reversible free radical mechanisms (not molecular mechanisms) to simulate the composition as a function of residence time. The main aim with the simulation model was to obtain a basic understanding of the formation and consumption of methane, ethane, ethene, ethyne and benzene in the temperature range 1200–1500°C with hydrogen dilution.

EXPERIMENTAL

A diagram of the experimental apparatus is shown in Fig. 1 [3–5]. The methane mixture (93% methane and 7% argon) and hydrogen were metered and mixed before entering the plug flow reactor. The reactor tube (sintered alumina) was 1200 mm long with an inner diameter of 9 mm.

The energy needed for the pyrolysis of methane was taken from an electric furnace (Kanthal) with the power input controlled manually by a Variac. The temperature was measured inside the reactor and in the air pocket in the furnace by Pt–Rh thermocouples. It was possible with this kind of furnace to increase the temperature up to 1600°C.

The product gases were rapidly quenched at the reactor outlet using a conical water-cooled cold finger forcing the gas through a narrow annulus with an opening of about 5 mm.

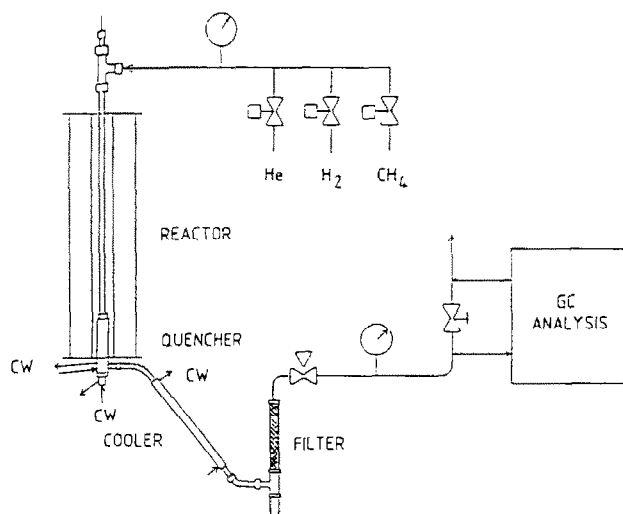


Fig. 1. Experimental apparatus for pyrolysis experiments.

Bourdon manometers were installed at the inlet and at the outlet of the reactor to measure the pressure inside the reactor and to see how the pressure changed over the reactor.

The product gases were analysed on-line by a gas chromatograph (HP 5890) which was equipped with a thermal conductivity detector (TCD) (Carbosieve S-88, packed 1/8 inch, 1.8 m long) and a flame ionization detector (FID) (Septa 77, GS-Q Megabore, internal diameter, 0.5 mm, length 10 m). Both detectors were connected to HP 3396 integrators. This allowed the analysis of CH₄, Ar (TCD) and CH₄, C₂H₆, C₂H₄, C₂H₂, C₆H₆ and other hydrocarbons (FID). Argon was used as an internal standard, and the mass balance was calculated. The difference in conversion of methane from the two methods (TC and FID) was ascribed to coke and tar formation.

The experiments were performed in series with constant feed gas composition and varying residence times or constant residence time and varying ratio between hydrogen and methane. Each condition was maintained for 10 min to obtain stable condition before an analysis was taken. The reactor was purged with H₂ at the reaction temperature between experimental points.

In the results benzene and higher hydrocarbons (coke) were lumped together and named benzene + “coke”.

THE SIMULATION MODEL

During the last few years simulation models have been used more and more in the scientific world. These simulation models can be divided into two categories, mechanistic and empirical models.

Like an empirical model, a mechanistic model explains experimental data and it also predicts results in a wide range of operational conditions which may be outside the range of experimental results. Such a model can be used to obtain a basic understanding of the system under study, to optimize the operation conditions and also to scale up the system.

A simulation model is in general based on three different parts.

(1) Description of the system: the type of reactor and a set of reaction mechanism.

(2) Translation of the chemical and physical problem, mass- and heat equations into mathematical terms.

(3) Numerical method to solve the system of balanced equations.

When comparing experimental data with a mathematical model of the system, the residuals between model prediction and observed data have three error sources: experimental error, error due to wrong parameter values in the model and error due to model inadequacy (choice of wrong reactor). It is of interest to minimize the residual error by a systematic search for the best model and the best parameter set in the chosen model.

In the present work the CHEMKIN code package [6] was used to simulate the process. This is a FORTRAN programme for predicting homogeneous gas phase chemical kinetics for different reactor systems. To simulate the experimental plug flow reactor a series of micromixed perfectly stirred reactors (PSR) [7] were used. The PSR code is not a stand-alone programme but is designed to be run in conjunction with the CHEMKIN code package. For each perfectly stirred reactor the system of algebraic equations was solved by the damped modified Newton algorithm [7].

In this modified CHEMKIN package a sensitivity analysis is included which was used for determining quantitatively how the solution of the model depended on certain parameters. In this way it was easier to tune the kinetic parameters and to see how important certain reaction pathways were for model predictions. Compared to repetitive running of the model the sensitivity analysis was significantly more efficient.

It is of interest to have the reaction scheme as simplified as possible, because it is easier to carry out careful adjustment of kinetic parameters. The species in the model were chosen from the experimental results where methane, ethane, ethene, ethyne and benzene played an important role. At the beginning, the model included about 60 reversible free radical reactions, but with use of the sensitivity analysis it was observed that some of these reactions had no influence on the main pathways. Thus, the resulting mechanism contained 32 reversible reactions and one irreversible reaction and can be seen in Table 1. The network is schematically described in Fig. 2.

Kinetic parameters were selected principally from Tsang and Hampson [8], but for some of the secondary reactions parameters from Zanthoff and Baerns [9], Dean [10], Isbarn *et al.* [11], Refael and Sher [12], Harris and Weiner [13], Ranzi *et al.* [2] and Westmoreland *et al.* [14] were used. The kinetic parameters have not been adjusted, except in reaction (1), where the frequency factor has been changed from $3.7 \times 10^{15} \text{ s}^{-1}$ to $3.5 \times 10^{15} \text{ s}^{-1}$, which is in the range of the recommended values reported by Tsang and Hampson [8]. This is a very small adjustment compared to the maximum range of adjustment of the kinetic parameters that Tsang and Hampson [8] have proposed.

We have made some simplifications in the model.

(1) The model lumps together the two possible structures for the radical C_4H_5



and



(2) The reaction (28) (see Table 1)

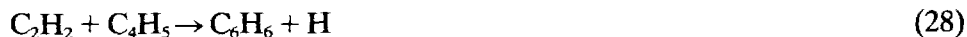


TABLE 1

Mechanisms, kinetic parameters^a and references

Reaction	Eqn.	A	n	B	Ref.
$\text{CH}_4 = \text{CH}_3 + \text{H}$	(1)	3.51×10^{15}	0.0	104000.0	8
$\text{CH}_4 + \text{H} = \text{CH}_3 + \text{H}_2$	(2)	2.25×10^4	3.0	8768.0	8
$\text{CH}_3 + \text{CH}_3 = \text{C}_2\text{H}_6$	(3)	1.01×10^{15}	-0.64	0.0	8
$\text{C}_2\text{H}_6 + \text{H} = \text{C}_2\text{H}_5 + \text{H}_2$	(4)	5.54×10^2	3.5	5174.0	8
$\text{C}_2\text{H}_6 + \text{CH}_3 = \text{C}_2\text{H}_5 + \text{CH}_4$	(5)	0.55	4.0	8296.0	8
$\text{C}_2\text{H}_5 = \text{C}_2\text{H}_4 + \text{H}$	(6)	2.00×10^{13}	0.0	39700.0	9
$\text{CH}_3 + \text{CH}_3 = \text{C}_2\text{H}_4 + \text{H}_2$	(7)	1.00×10^{16}	0.0	32000.0	9
$\text{C}_2\text{H}_4 + \text{CH}_3 = \text{C}_2\text{H}_3 + \text{CH}_4$	(8)	6.62	3.7	9512.0	8
$\text{C}_2\text{H}_4 + \text{CH}_3 = \text{N}^*\text{C}_3\text{H}_7$	(9)	3.31×10^{11}	0.0	7715.0	8
$\text{C}_2\text{H}_4 + \text{H} = \text{C}_2\text{H}_3 + \text{H}_2$	(10)	1.32×10^6	2.53	12258.0	8
$\text{C}_2\text{H}_3 = \text{C}_2\text{H}_2 + \text{H}$	(11)	1.93×10^{28}	-4.783	51123.0	10
$\text{CH}_3 + \text{C}_2\text{H}_3 = \text{C}_3\text{H}_6$	(12)	1.00×10^{13}	0.0	0.0	9
$\text{N}^*\text{C}_3\text{H}_7 = \text{C}_3\text{H}_5 + \text{H}$	(13)	1.58×10^{16}	0.0	38000.0	9
$\text{C}_3\text{H}_6 = \text{C}_3\text{H}_5 + \text{H}$	(14)	1.00×10^{15}	0.0	88000.0	11
$\text{C}_3\text{H}_5 = \text{C}_2\text{H}_2 + \text{CH}_3$	(15)	3.16×10^{10}	0.0	36200.0	11
$\text{C}_3\text{H}_5 = \text{C}_3\text{H}_4 + \text{H}$	(16)	5.00×10^9	0.0	35000.0	12
$\text{C}_3\text{H}_5 + \text{H} = \text{C}_3\text{H}_4 + \text{H}_2$	(17)	1.00×10^{13}	0.0	0.0	12
$\text{C}_3\text{H}_6 + \text{H} = \text{C}_3\text{H}_5 + \text{H}_2$	(18)	3.16×10^{11}	0.0	4500.0	11
$\text{C}_2\text{H}_3 + \text{C}_2\text{H}_3 = \text{C}_4\text{H}_6$	(19)	1.26×10^{13}	0.0	0.0	11
$\text{C}_2\text{H}_3 + \text{C}_2\text{H}_4 = \text{C}_4\text{H}_6 + \text{H}$	(20)	5.00×10^{11}	0.0	7315.0	8
$\text{C}_2\text{H}_2 + \text{H} = \text{C}_2\text{H} + \text{H}_2$	(21)	6.02×10^{13}	0.0	22300.0	8
$\text{C}_2\text{H}_2 + \text{CH}_3 = \text{C}_2\text{H} + \text{CH}_4$	(22)	1.81×10^{11}	0.0	17300.0	8
$\text{C}_4\text{H}_6 + \text{H} = \text{C}_4\text{H}_5 + \text{H}_2$	(23)	1.00×10^{14}	0.0	15000.0	13
$\text{C}_4\text{H}_5 = \text{C}_4\text{H}_4 + \text{H}$	(24)	1.00×10^{14}	0.0	41400.0	13
$\text{C}_2\text{H} + \text{H} = \text{C}_2\text{H}_2$	(25)	1.81×10^{14}	0.0	0.0	8
$\text{C}_2\text{H}_3 + \text{C}_2\text{H}_2 = \text{C}_4\text{H}_5$	(26)	1.10×10^{12}	0.0	4000.0	2
$\text{CH}_3 + \text{CH}_3 = \text{C}_2\text{H}_5 + \text{H}$	(27)	1.80×10^{12}	0.0	10400.0	10
$\text{C}_4\text{H}_5 + \text{C}_2\text{H}_2 = \text{C}_6\text{H}_6 + \text{H}$	(28)	6.02×10^{12}	0.0	9000.0	14
$\text{C}_2\text{H}_4 + \text{C}_2\text{H}_2 + \text{H}$	(29)	1.00×10^{16}	0.0	108000.0	11
$\text{C}_2\text{H}_5 + \text{C}_2\text{H}_2 = \text{C}_2\text{H}_6 + \text{C}_2\text{H}$	(30)	2.71×10^{11}	0.0	23400.0	8
$\text{C}_2\text{H}_5 + \text{H} = \text{C}_2\text{H}_6$	(31)	3.07×10^{13}	0.0	0.0	8
$\text{C}_2\text{H}_4 = \text{C}_2\text{H}_2 + \text{H}_2$	(32)	7.94×10^{12}	0.44	88760.0	8
$\text{C}_2\text{H}_3 + \text{H} = \text{C}_2\text{H}_2 + \text{H}_2$	(33)	9.64×10^{13}	0.0	0.0	8

^a Kinetic parameters use the units cm^3 , moles, seconds and kcal.

is irreversible; all other reactions in the model are reversible. The model does not describe in detail the formation of higher aromatics and coke. In the results C_6H_6 and higher hydrocarbons are lumped together and called C_6H_6 + “coke”.

Because of these two simplifications the model has lost some information at high conversion, but the purpose is to obtain a good model for the formation and consumption of methane, ethane, ethene, ethyne and benzene in the temperature range 1200–1500°C with hydrogen dilution.

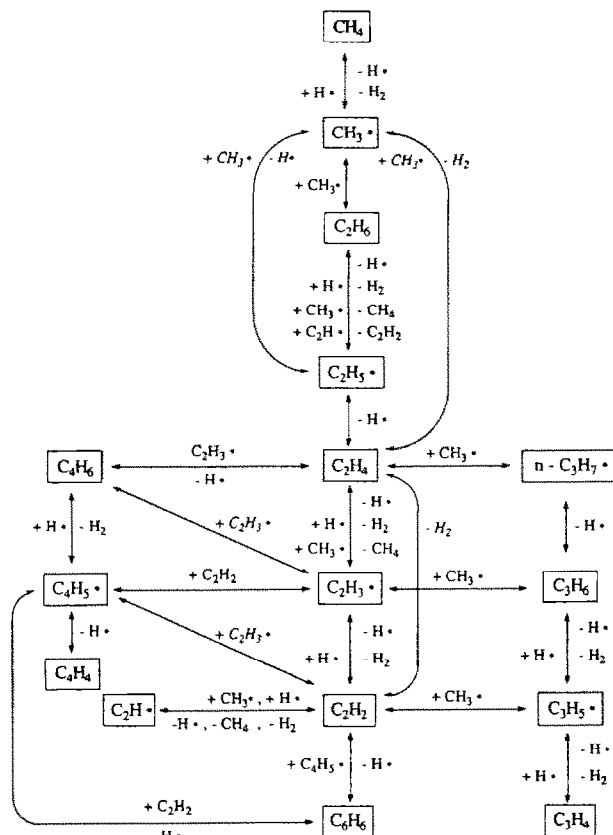


Fig. 2. Block diagram of the reaction network in the model.

RESULTS AND DISCUSSION

Figures 3–6 show the selectivity of ethene, ethyne, C_6H_6 + “coke” and the conversion of methane as a function of residence time for the conditions being modelled. Also shown in these figures are experimental data for the three products reported and data for the conversion of methane.

The chosen simulation temperature (T_{sim}) was lower than the maximal measured temperature (T_{max}) in the reactor. A general agreement has been reached by using a simulation temperature between 50 and 100°C lower than the maximal measured temperature in the reactor, respectively 1150°C ($T_{max} = 1200^\circ C$), 1240°C ($T_{max} = 1300^\circ C$), 1300°C ($T_{max} = 1400^\circ C$) and 1400°C ($T_{max} = 1500^\circ C$). The reason for doing this was the temperature difference between the reactor wall (measured temperature) and the bulk of the gas. This lowering of the simulation temperature to fit experimental data have also been carried out by Ranzi et al. [2].

The agreement between simulated and experimental data was good, especially in the middle of the time range. According to Figs. 5 and 6 there

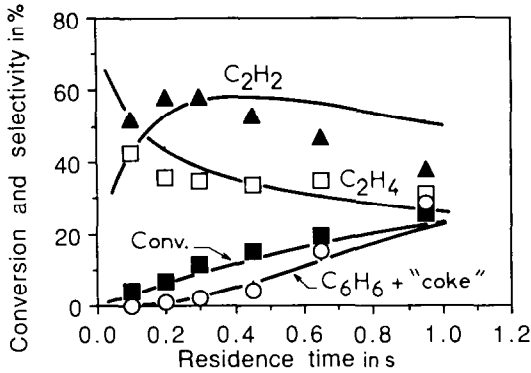


Fig. 3. Selectivity of products and conversion of methane from methane pyrolysis as a function of residence time. Pressure 1 atm. Feed composition $H_2:CH_4 = 2:1$. Maximal temperature in the reactor $1200^\circ C$ ($T_{sim} = 1150^\circ C$). Solid lines are simulated data and experimental data are indicated by plotting symbols: ■, conversion; □, C_2H_4 ; ▲, C_2H_2 ; ○, $C_6H_6 + \text{"coke"}$.

were, however, some differences between simulated and experimental data at very short residence time. It may be suggested that this difference was due to error in the calculation of the residence time in the reactor. When the residence time was very short, the gas mixture passed through the reactor tube very quickly. When the gas flow increased, the temperature profile in the reactor tube changed and the average temperature in the reactor decreased. This phenomenon was not taken into account when the experimental residence time was calculated.

In Figs. 7–10 the selectivity of the products, for the model data, was

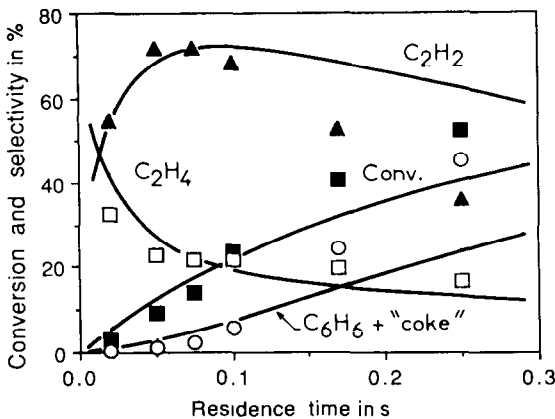


Fig. 4. Selectivity of products and conversion of methane from methane pyrolysis as a function of residence time. Pressure 1 atm. Feed composition $H_2:CH_4 = 2:1$. Maximal temperature in the reactor $1300^\circ C$ ($T_{sim} = 1240^\circ C$). Solid lines are simulated data and experimental data are indicated by plotting symbols: ■, conversion; □, C_2H_4 ; ▲, C_2H_2 ; ○, $C_6H_6 + \text{"coke"}$.

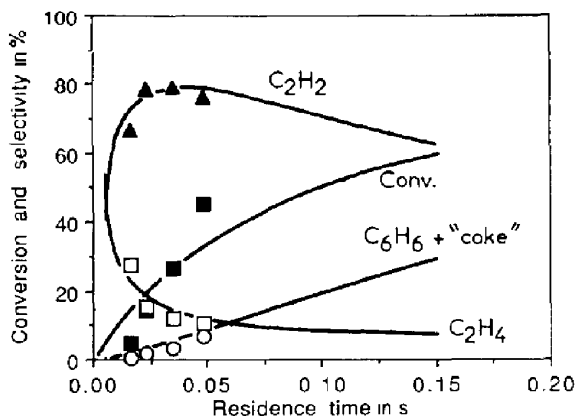


Fig. 5. Selectivity of products and conversion of methane from methane pyrolysis as a function of residence time. Pressure 1 atm. Feed composition $\text{H}_2:\text{CH}_4 = 2:1$. Maximal temperature in the reactor 1400°C ($T_{\text{sim}} = 1300^\circ\text{C}$). Solid lines are simulated data and experimental data are indicated by plotting symbols: ■, conversion; □, C_2H_4 ; ▲, C_2H_2 ; ○, $\text{C}_6\text{H}_6 + \text{"coke"}$.

plotted as a function of the conversion of methane. These figures also show experimental data for the reported products. It can be seen that the agreement between model data and experimental data was better when the selectivities of the products were plotted as a function of conversion. Thus, the time factor was eliminated.

Figures 3 and 4 show that the simulated values for the selectivity of ethyne were too high and the simulated values for $\text{C}_6\text{H}_6 + \text{"coke"}$ were too

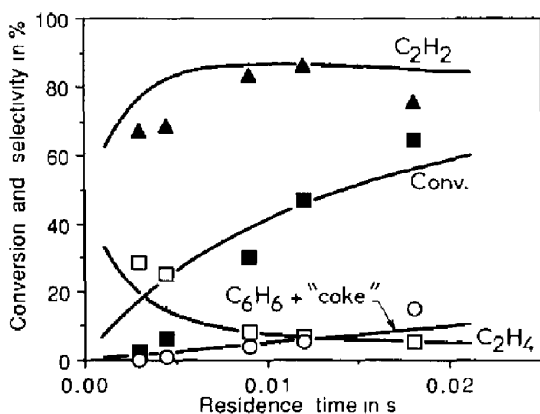


Fig. 6. Selectivity of products and conversion of methane from methane pyrolysis as a function of residence time. Pressure 1 atm. Feed composition $\text{H}_2:\text{CH}_4 = 2:1$. Maximal temperature in the reactor 1500°C ($T_{\text{sim}} = 1400^\circ\text{C}$). Solid lines are simulated data and experimental data are indicated by plotting symbols: ■, conversion; □, C_2H_4 ; ▲, C_2H_2 ; ○, $\text{C}_6\text{H}_6 + \text{"coke"}$.

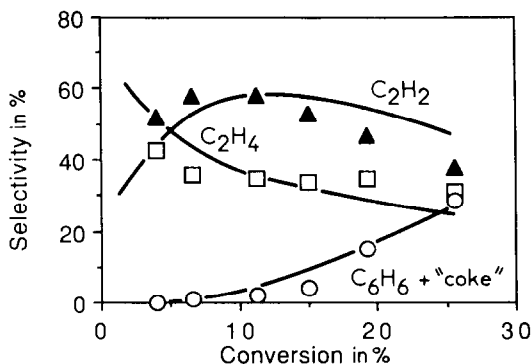


Fig. 7. Selectivity of products from pyrolysis of methane as a function of the conversion of methane. Pressure 1 atm. Feed composition $\text{H}_2:\text{CH}_4 = 2:1$. Maximal temperature in the reactor tube 1200°C ($T_{\text{sim}} = 1150^\circ\text{C}$). Solid lines are simulated data and experimental data are indicated by plotting symbols: \square , C_2H_4 ; \blacktriangle , C_2H_2 ; \circ , C_6H_6 + "coke".

low at high residence times. This may be explained by some incompleteness in the model for the C_4H_5 radical and in reaction (28) (see Table 1) in the formation of C_6H_6



New reactions and species have to be introduced into the model for improving the simulated data at high conversions where the rate of "coke" formation was very high.

Figure 11 shows the conversion of methane as a function of residence time with different ratios between hydrogen and methane for the experimental data. In Fig. 12 the same is shown for simulated data.

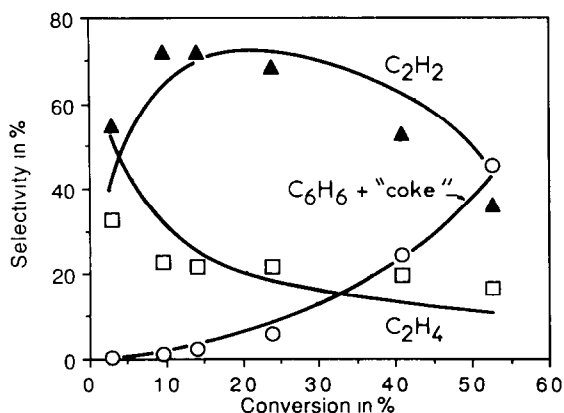


Fig. 8. Selectivity of products from pyrolysis of methane as a function of the conversion of methane. Pressure 1 atm. Feed composition $\text{H}_2:\text{CH}_4 = 2:1$. Maximal temperature in the reactor 1300°C ($T_{\text{sim}} = 1240^\circ\text{C}$). Solid lines are simulated data and experimental data are indicated by plotting symbols: \square , C_2H_4 ; \blacktriangle , C_2H_2 ; \circ , C_6H_6 + "coke".

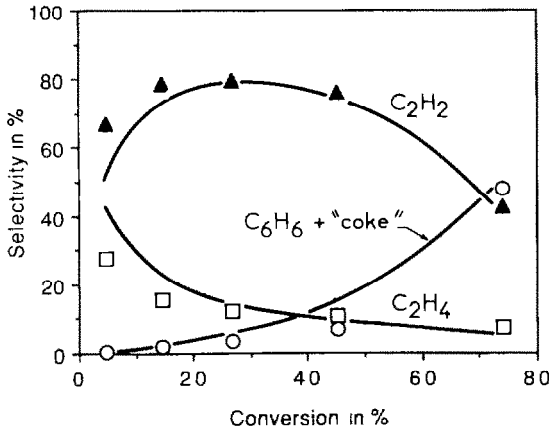


Fig. 9. Selectivity of products from pyrolysis of methane as a function of the conversion of methane. Pressure 1 atm. Feed composition $\text{H}_2:\text{CH}_4 = 2:1$. Maximal temperature in the reactor tube 1400°C ($T_{\text{sim}} = 1300^\circ\text{C}$). Solid lines are simulated data and experimental data are indicated by plotting symbols: \square , C_2H_4 ; \blacktriangle , C_2H_2 ; \circ , C_6H_6 + "coke".

It can be seen from these two figures that there was good agreement of the tendencies between the model and the experimental data. When the ratio between hydrogen and methane increased, the conversion of methane decreased, and these results were in agreement with the results presented by Ranzi et al. [2].

MECHANISMS

Product rate coefficients for species j are defined as

$$C_{i,j} = \frac{r_{i,j}}{|\sum r_{i,j}|}$$

where $r_{i,j}$ is the rate of reaction i in the production (consumption) of species j , and $\sum r_{i,j}$ is the sum of all the rates for all the reactions taking part in the production (consumption) of species j . Production rates give positive values, and consumption rates give negative values.

Tables 2–5 show the production rate coefficients for the main compounds in the pyrolysis of methane at two different temperatures ($T_{\text{sim}} = 1150^\circ\text{C}$ and 1400°C) and two different conversions (2.1% and 8.9%).

It can be seen from Table 2 that the two reactions



and



are the only important reactions in the consumption of CH_4 and in the

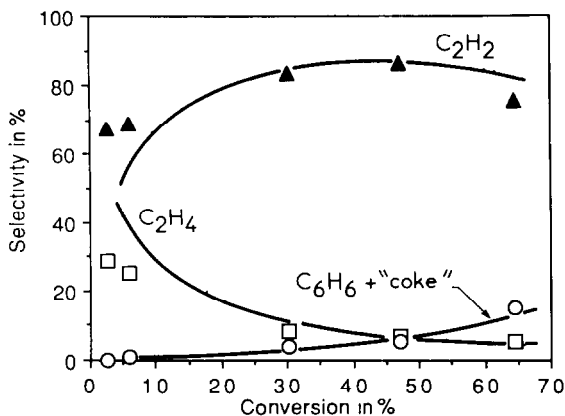


Fig. 10. Selectivity of products from pyrolysis of methane as a function of the conversion of methane. Pressure 1 atm. Feed composition $\text{H}_2:\text{CH}_4 = 2:1$. Maximal temperature in the reactor tube 1500°C ($T_{\text{sm}} = 1400^\circ\text{C}$). Solid lines are simulated data and experimental data are indicated by plotting symbols: \square , C_2H_4 ; \blacktriangle , C_2H_2 ; \circ , C_6H_6 + "coke".

formation of the radical CH_3 . Reaction (2) is the most important of the two under all conditions, and the difference between the two reactions decreases with increasing temperature at 2.1% conversion. The same effect cannot be observed at 8.9% conversion. Table 2 shows that reaction (2) becomes more important, compared with reaction (1), when the conversion increases. The same table shows that the net rate of production ($\text{mol cm}^{-3} \text{s}^{-1}$) and the net rate of consumption ($\text{mol cm}^{-3} \text{s}^{-1}$) were around 200 times faster at the highest temperature compared to the lowest temperature.

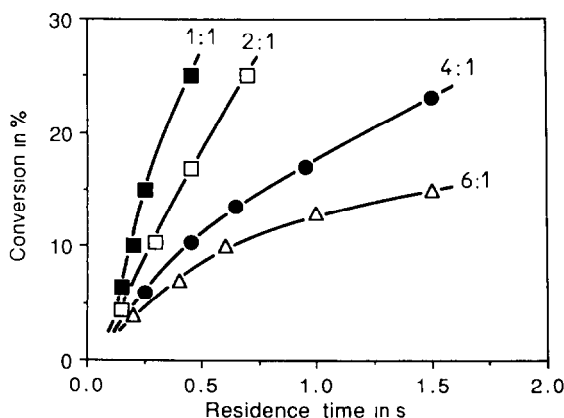


Fig. 11. Conversion of methane, for different feed compositions between H_2 and CH_4 , as a function of residence time. Maximal temperature in the reactor tube 1200°C . Pressure 1 atm. The different ratios between H_2 and CH_4 are indicated by the following symbols: Δ , 6:1; \bullet , 4:1; \square , 2:1; \blacksquare , 1:1.

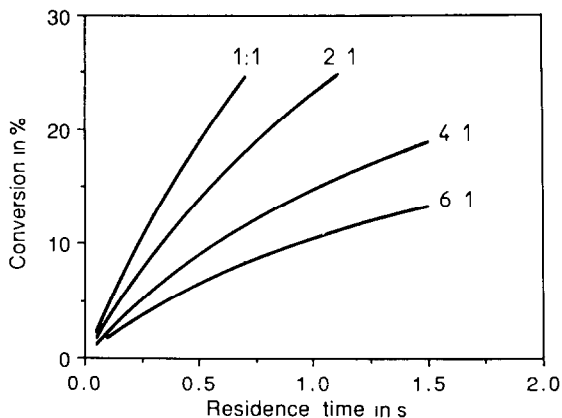


Fig. 12. The simulated conversion of methane, for different feed compositions between H_2 and CH_4 , as a function of residence time. Simulated temperature $1150^\circ C$. Pressure 1 atm.

The reaction



is the only one in which C_2H_6 is produced. This confirms the proposition by Back and Back [15] that C_2H_6 is produced by a termination of two CH_3 radicals.

The two important reactions in the formation of the radical C_2H_5 are



and



Table 3 shows that hydrogen abstraction by the H radical is more dominant

TABLE 2

Sensitivity analysis for the consumption and production of methane

Reaction	Eqn. ^a	Normalized rate of production coefficients			
		1150°C		1400°C	
		2.10 ^b	8.90 ^b	2.10 ^b	8.90 ^b
$CH_4 = CH_3 + H$	(1)	-0.426	-0.391	-0.445	-0.391
$CH_4 + H = CH_3 + H_2$	(2)	-0.574	-0.609	-0.555	-0.609
$C_2H_6 + CH_3 = C_2H_5 + CH_4$	(5)	0.477	0.477	0.561	0.300
$C_2H_4 + CH_3 = C_2H_3 + CH_4$	(8)	0.523	0.523	0.438	0.700
Net rate of production in moles $cm^{-3}s^{-1}$		1.18×10^{-7}	1.22×10^{-7}	1.31×10^{-5}	2.35×10^{-5}
Net rate of consumption in moles $cm^{-3}s^{-1}$		1.08×10^{-6}	8.74×10^{-7}	2.16×10^{-4}	1.76×10^{-4}

^a See Table 1. ^b Conversion percentage.

TABLE 3
Sensitivity analysis for the production and consumption of ethane

Reaction	Eqn. ^a	Normalized rate of production coefficients			
		1150°C		1400°C	
		2.10 ^b	8.90 ^b	2.10 ^b	8.90 ^b
$2\text{CH}_3 = \text{C}_2\text{H}_6$	(3)	1.000	1.000	1.000	1.000
$\text{C}_2\text{H}_6 + \text{H} = \text{C}_2\text{H}_5 + \text{H}_2$	(4)	-0.865	-0.877	-0.798	-0.815
$\text{C}_2\text{H}_6 + \text{CH}_3 = \text{C}_2\text{H}_5 + \text{CH}_4$	(5)	-0.124	-0.112	-0.149	-0.136
$\text{C}_2\text{H}_5 + \text{H} = \text{C}_2\text{H}_6$	(31)	-0.011	-0.012	-0.052	-0.049
Net rate of production in moles $\text{cm}^{-3} \text{s}^{-1}$		4.54×10^{-7}	3.57×10^{-7}	6.32×10^{-5}	5.14×10^{-5}
Net rate of consumption in moles $\text{cm}^{-3} \text{s}^{-1}$		4.53×10^{-7}	3.57×10^{-7}	4.91×10^{-5}	5.18×10^{-5}

^a See Table 1. ^b Conversion percentage.

than the hydrogen abstraction by the CH_3 radical, even though the concentration of the H radical is almost 10 times lower than the concentration of the CH_3 radical. This shows the high reactivity of the H radical.

Table 4 shows the production rate coefficients for the production and consumption of C_2H_4 . It can be seen that at 1150°C, both for low and high conversions, the dominant reaction is



TABLE 4
Sensitivity analysis for the production and consumption of ethene

Reaction	Eqn. ^a	Normalized rate of production coefficients			
		1150°C		1400°C	
		2.10 ^b	8.90 ^b	2.10 ^b	8.90 ^b
$\text{C}_2\text{H}_5 = \text{C}_2\text{H}_4 + \text{H}$	(6)	0.963	0.965	0.690	0.712
$2\text{CH}_3 = \text{C}_2\text{H}_4 + \text{H}_2$	(7)	0.037	0.035	0.310	0.288
$\text{C}_2\text{H}_4 + \text{CH}_3 = \text{C}_2\text{H}_3 + \text{CH}_4$	(8)	-0.269	-0.263	-0.263	-0.258
$\text{C}_2\text{H}_4 + \text{CH}_3 = \text{N}^* \text{C}_3\text{H}_7$	(9)	-0.032	-0.030	-0.043	-0.029
$\text{C}_2\text{H}_4 + \text{H} = \text{C}_2\text{H}_3 + \text{H}_2$	(10)	-0.370	-0.412	-0.345	-0.378
$\text{C}_2\text{H}_4 = \text{C}_2\text{H}_3 + \text{H}$	(20)	-0.011	-0.15	-0.027	-0.024
$\text{C}_2\text{H}_4 = \text{C}_2\text{H}_2 + \text{H}_2$	(32)	-0.318	-2.80	-0.321	-0.311
Net rate of production in moles $\text{cm}^{-3} \text{s}^{-1}$		4.77×10^{-7}	3.76×10^{-7}	7.52×10^{-5}	7.65×10^{-5}
Net rate of consumption in moles $\text{cm}^{-3} \text{s}^{-1}$		2.29×10^{-7}	3.12×10^{-7}	2.17×10^{-5}	6.38×10^{-5}

^a See Table 1. ^b Conversion percentage.

TABLE 5

Sensitivity analysis for the production and consumption of ethyne

Reaction	Eqn. ^a	Normalized rate of production coefficients			
		1150°C		1400°C	
		2.10 ^b	8.90 ^b	2.10 ^b	8.90 ^b
$C_2H_3 = C_2H_2 + H$	(11)	0.657	0.666	0.641	0.651
$C_3H_5 = C_2H_2 + CH_3$	(15)	0.011	0.015	0.010	0.011
$C_2H_3 + C_2H_2 = C_4H_5$	(26)	-0.500	-0.500	-0.724	-0.502
$C_4H_5 + C_2H_3 = C_6H_6 + H$	(28)	-0.499	-0.500	-0.254	-0.494
$C_2H_4 = C_2H_2 + H_2$	(32)	0.324	0.317	0.329	0.315
$C_2H_2 + H = C_2H + H_2$	(21)	0.000	0.000	-0.018	0.000
$C_2H_3 + H = C_2H_2 + H_2$	(33)	0.000	0.000	0.020	0.022
Net rate of production in moles $cm^{-3} s^{-1}$		2.25×10^{-7}	2.76×10^{-7}	2.11×10^{-5}	6.29×10^{-5}
Net rate of consumption in moles $cm^{-3} s^{-1}$		3.77×10^{-9}	7.17×10^{-8}	2.15×10^{-8}	1.08×10^{-6}

^a See Table 1. ^b Conversion percentage.

At 1400°C the reaction



also becomes important.

For the production of the radical C_2H_3 there are two main elementary reactions

and



It can also be seen from Table 4 that the reaction



has larger influence at the highest temperature compared to the lowest temperature, and may be at even higher temperatures this reaction becomes dominant. This is in agreement with the thermodynamics which say that the C–H bond in C_2H_4 (molecular decomposition of C_2H_4) needs more energy than the competitive abstraction reactions before it can be broken.

There are two dominant reactions in the production of C_2H_2 

and



where reaction (11) is the most important at both high and low conversions and at both the temperatures studied.

ACKNOWLEDGEMENTS

The authors are grateful to the Royal Norwegian Council for Scientific and Industrial Research for financial support through the SPUNG program. We thank the French company Total A/S Marine for financial support.

REFERENCES

- 1 F. Billaud, F. Baronnet, E. Freund, C. Busson and J. Weill, *Rev. Inst. Fr. Pét. Ann. Combust. Liq.*, 44 (1989) 813.
- 2 E. Ranzi, M. Dente, M. Costa and V. Bruzzi, *Ing. Chim. Ital.*, 24 (1988) 1.
- 3 O.A. Rokstad, O. Olsvik, B. Jensen and A. Holmen, in L.F. Albright, B.L. Crynes and S. Nowak (Eds.), *Novel Methods of Producing Ethylene, Other Olefins and Aromatics*, Marcel Dekker, New York, 1992, pp. 259–272.
- 4 O.A. Rokstad, O. Olsvik and A. Holmen, *Natural gas conversion*, in A. Holmen, K.-J. Jens and S. Kolboe (Eds.), *Stud. Surf. Sci. Catal.*, Elsevier, Amsterdam, 1991, p. 533.
- 5 E.A. Blekkan, R. Myrstad, O. Olsvik and O.A. Rokstad, *Carbon*, 30 (1992) 665.
- 6 R.J. Kee, J.A. Miller and T.H. Jefferson, *CHEMKIN: A General Purpose, Problem-Independent Transportable, FORTRAN Chemical Kinetics Code Package*, Sandia National Laboratory Report, SAND 80-8003 (1980).
- 7 P. Glarborg, R.J. Kee, J.F. Grear and J.A. Miller, *PSR: A FORTRAN Program for Modeling Well-Stirred Reactors*, Sandia National Laboratory Report, SAND 86-8209 (1986).
- 8 W. Tsang and R.F. Hampson, *J. Phys. Chem. Ref. Data*, 15 (1986) 1087.
- 9 H. Zanthoff and M. Baerns, *Ind. Eng. Chem. Res.*, 29 (1990) 2.
- 10 A.M. Dean, *J. Phys. Chem.*, 94 (1990) 1432.
- 11 G. Isbarn, H.J. Ederer and K.H. Ebert, *Chem. Phys.*, 18 (1981) 241.
- 12 S. Refael and E. Sher, *Combust. Flame*, 78 (1989) 326.
- 13 S.J. Harris and S.M. Weiner, *Combust. Flame*, 72 (1988) 91.
- 14 P.R. Westmoreland, A.M. Dean, J.B. Howard and J.P. Longwell, *J. Phys. Chem.*, 93 (1989) 8171.
- 15 M.H. Back and R.A. Back, in L.F. Albright, B.L. Crynes and W.H. Corcoran, (Eds.), *Pyrolysis: Theory and Industrial Practice*, Academic Press, New York, 1983.